



# Groundwater quality assessment for sustainable human consumption in arid areas based on GIS and water quality index in the watershed of Ain Sefra (SW of Algeria)

Derdour Abdessamed<sup>1,2</sup> · Antonio Jodar-Abellan<sup>3,4,5</sup> · Sherif S. M. Ghoneim<sup>6</sup> · Abdulrazak Almaliki<sup>8</sup> · Enas E. Hussein<sup>7</sup> · Miguel Ángel Pardo<sup>5</sup>

Received: 22 June 2022 / Accepted: 8 September 2023  
© The Author(s) 2023

## Abstract

Groundwater quality in arid areas is an issue that requires attention, as often the only source of irrigation and drinking. In this manuscript, a research area of 4590.2 Km<sup>2</sup>, which depicts important problems of water scarcity and water-poor quality in an arid environment, was assessed. Therefore, GIS-based mapping of the region was carried out to examine the adequacy of groundwater quality. Forty-three (43) groundwater samples were gathered in the fieldwork in March 2022, and various physicochemical limits were analysed within Gibbs and Piper diagrams. Likewise, spatial distribution maps of twelve (12) main water quality parameters were performed using the Inverse Distance Weighted interpolation method (IDW) in the ArcGIS tool. The Water Quality Index (WQI) has been calculated considering Algerian drinking water quality standards and to know the suitability of water for human consumption. A Pearson's test was carried out to explore the correlations among the different variables. Major results of the study showed that, among anions and cations, sulphates ( $SO_4^{2-}$ ) and calcium (Ca) were the most common ions. The WQI showed that 30.23% of the samples have excellent water quality, 62.79% belong to the good water category, and 6.97% fall into the poor water quality category. Thus, the correlation study between many physicochemical properties also showed significant positive relationships between WQI, TDS, EC, TH,  $SO_4^{2-}$ ,  $Ca^{++}$ , and  $Mg^{++}$ . In agreement with the Gibbs diagram, most of the samples fall into the field of rock-water interaction dominance. Hence, this research shows that using GIS and WQI as joint approaches could be useful tools for the decision-making process of local and international authorities and water resources management.

**Keywords** WQI · Potability · IDW · Gibbs diagram · Piper diagram · Ain Sefra

✉ Miguel Ángel Pardo  
mpardo@ua.es  
Derdour Abdessamed  
derdour@cuniv-naama.dz  
Antonio Jodar-Abellan  
ajodar@cebas.csic.es  
Sherif S. M. Ghoneim  
s.ghoneim@tu.edu.sa  
Abdulrazak Almaliki  
a.almaliki@tu.edu.sa  
Enas E. Hussein  
enas\_el-sayed@nwrc.gov.eg

<sup>3</sup> Centro de Investigación e Innovación Agroalimentaria y Agroambiental (CIAGRO-UMH), Miguel Hernandez University, Ctra. Beniel Km 3.2, 03312 Orihuela, Spain  
<sup>4</sup> Centro de Edafología y Biología Aplicada del Segura (CEBAS-CSIC), Soil and Water Conservation Group, Spanish Research Council, Murcia, Spain  
<sup>5</sup> Department of Civil Engineering, University of Alicante, Alicante, Spain  
<sup>6</sup> Department of Electrical Engineering, College of Engineering, Taif University, Taif, Saudi Arabia  
<sup>7</sup> National Water Research Center, Cairo, Egypt  
<sup>8</sup> Department of Civil Engineering, College of Engineering, Taif University, P.O. BOX 11099, Taif 21944, Saudi Arabia

<sup>1</sup> Laboratory for the Sustainable Management of Natural Resources in Arid and Semi-arid Zones, University Center Salhi Ahmed Naama, Naama, Algeria

<sup>2</sup> Artificial Intelligence Laboratory for Mechanical and Civil Structures, and Soil, University Center of Naama, P.O. Box 66, 45000 Naama, Algeria

## Introduction

Millions of human beings around the globe face water scarcity and suffer to meet their needs daily (García-López et al. 2022; Moussaoui et al. 2023). Water-related natural disasters, such as tropical storms, floods, and tsunamis, cause much loss of life and suffering (Annan 2005; Jodar-Abellan et al. 2019). All too often, drought strikes the world's poorest countries, aggravating hunger and malnutrition (Annan 2005). Accessibility to safe and inexpensive drinking water is an elementary human need and a fundamental right (Hartmann et al. 2013; Russell 2010). For most of the population in arid areas in Algeria, groundwater is the dominant supply for human consumption (Kendouci et al. 2019).

Groundwater dependence has increased because of population growth, agriculture, urbanisation, and changing lifestyles which must be studied, furthermore, in the context of the current climate change (Nath et al. 2021; Pardo et al. 2022; Eekhout et al. 2021). Groundwater resources suffer from these problems, both in quantity and quality (Chakraborty et al. 2021; Boix-Fayos et al. 2020; Valdes-Abellan et al. 2020). Accessibility and quantity of drinking water are nothing without quality, as poor-quality drinking water leads to health problems that can even cause death (Karandish et al. 2018; Tian et al. 2019). When chemicals, such as nitrates and sulphates, exceed permissible drinking limits, they can cause chronic health effects (Prüss-Ustün et al. 2019; Kumar et al. 2023). In semi-arid and arid regions, agriculture has a major influence on groundwater quality because of chemical fertilisers (Wada et al. 2012). Therefore, the chemical quality of drinking water—whether from groundwater or surface water—should be checked before being delivered to consumers. The physical quality of drinking water affects its aesthetic value and acceptability, which often goes with the sociocultural beliefs of consumers. Groundwater quality in a particular area depends on natural or anthropogenic factors (Long et al. 2021; Tian et al. 2019).

The geology and the age of the water in the aquifer offer information on the velocity and dispersion of contaminants in the aquifer (Davie et al. 2008). Thus, water quality is assessed by its chemical, biological, aesthetic, and physical aspects (Pla et al. 2021; Chakraborty et al. 2021). As water has a variety of uses and purposes, each type of water has its own specific needs, standards, and guidelines. The World Health Organization (WHO) Drinking Water Guidelines define acceptable smallest threshold safety criteria to preserve consumers' health and set up "guideline values" for all water elements (WHO 2011; Kumar et al. 2023). However, WHO recognizes many other situations (cultural, economic, social, etc.) that may dictate other mandatory limits and thus give rise to national, local, or regional standards. Hence, the diversity of drinking water standards is clear, as no single

universally applicable approach to drinking water standards (WHO 2011; Tian et al. 2019). Unfortunately, the WHO does not advocate adopting international drinking-water quality standards, because the conditions that force adopting other standards may impose even poorer quality. Thus, Algeria presents the Algerian water Standards (AS), used by international and regional standards. These are applied in particular tests and analytical specifications on drinking water (JORADP 2011). Therefore, water is unfit for consumption when the physico-chemical constituents of water resources exceed international or national standards or regulations.

The Water Quality Index (WQI), described by Horton et al. (1965) and developed by Brown et al. (1972), is an important indicator for assessing water quality. In this index, several chemical parameters are considered, with various weightings, to offer a set of results that find the quality of a specific water sample (Jehan et al. 2020; Rabeiy 2018; Ramos et al. 2016). Over the past decades, many studies worldwide highlighted the WQI technique's effectiveness in describing and assessing water quality. The WQI approach has been used to assess groundwater quality in many regions (Gradilla-Hernández et al. 2020; Lumb et al. 2011; Rabeiy 2018; Wang et al. 2018) because of its ability to assess and manage water quality indicators (de Almeida et al. 2018; Song and Yao 2022). Earlier research was limited in scope: Sadat-Noori et al. (2014) used the Water Quality Index in Iran without going into the relationships between the chemical elements and their dynamics; Nong et al. (2020) studied microbiological limits in the trans-basin river in China, etc.; Rao et al. (2013) used 7 parameters to assess the water quality in Visakhapatnam in India; Derdour et al. (2020) and Derdour et al. (2021) studied the WQI in small watersheds without using Gibbs and Piper plots. Therefore, it should be noted that an important lack of scientific studies covering the manuscript's topic in arid areas was identified. The water quality in this area has not been studied before. However, our approach suffers from limitations because of the lack of microbiological analysis data and the difficult access to boreholes in the Algerian-Moroccan borders. The method presented in this work applies to other arid regions.

Many researchers have used Geographical Information System (GIS) and Inverse Distance-Weighted (IDW) algorithms to present the Water Quality Index (WQI) (El Behairy et al. 2021). This method enables researchers to display the spatial distribution of groundwater quality and to find areas with poor water quality (Chabuk et al. 2020; Kawo et al. 2018). The IDW algorithm interpolates water quality data from sampling points to a continuous map, while the GIS provides a visual representation of the data, facilitating interpretation and analysis. Thus, the WQI provides a comprehensive assessment of groundwater quality by combining several water quality parameters into a single index, allowing

for an easy comparison and assessment of groundwater quality in different regions (Li et al. 2021; Hinge et al. 2022).

This work was performed in the Ain Sefra catchment area, part of the Ksour Mountains region, in the southwest of Algeria, on the border with Morocco. This site depends on the groundwater supply, as groundwater is the only support for drinking water and agricultural water (Derdour et al. 2021). Thus, the Ain Sefra basin is where this study needs to be developed. The central aims of this study are: (i) evaluate the physico-chemical properties of the study area; (ii) show the origin of groundwater using Piper and Gibbs diagrams; (iii) find the water quality in the Ain Sefra basin using WQI analysis. Finally, obtained results were assessed and compared with Algerian standards for water quality recommendations.

## Materials and methods

### Overview of the study area

The area selected for this study was the Ain Sefra catchment (also known as ‘Upper Wadi Namous ‘), in south-western

Algeria in a border region called “Ksour Mountains” (Fig. 1). It lies between latitudes (32°15'25.09"N and 33°5'33.78"N) and longitudes (1°2'52.84"W and 0°6'8.08"W). This region covers an area of 4590.2 Km<sup>2</sup>, representing about 15.4% of the total area of Wilaya of Naâma (Derdour & Bouanani 2019). This basin comprises 05 administrative units (known as ‘communes: Ain Sefra, Sfissifa, Moghrar, Djenien Bourezg, and Tiout).

The altitude ranges between 804.5 m and 2219.4 m above sea level (m.a.s.l). Medium and low slopes characterise the relief of the region. Because of its geographical location, the region has arid to semi-arid climatic conditions, and hydrological behaviour is characterised by spatial and temporal variability (Derdour et al. 2019). Morphologically, the Ksour Mountains are distinguished by their very high reliefs, with peaks reaching an altitude of over 2000 m.a.s.l (Djebel Aissa, 2236 m.a.s.l; M'zi, 2167 m.a.s.l, and Mir El Djebel, 2109 m.a.s.l), dotted with small valleys and alluvial terraces occupied by oases like Tiout, Moghrar, Sfissifa and Asla. The principal towns besides Ain Sefra are Tiout, Sfissifa, Moghrar, and Djenien Bourezg. The stratigraphic series in the study area ranges from the Triassic to the recent Quaternary (Fig. 2).

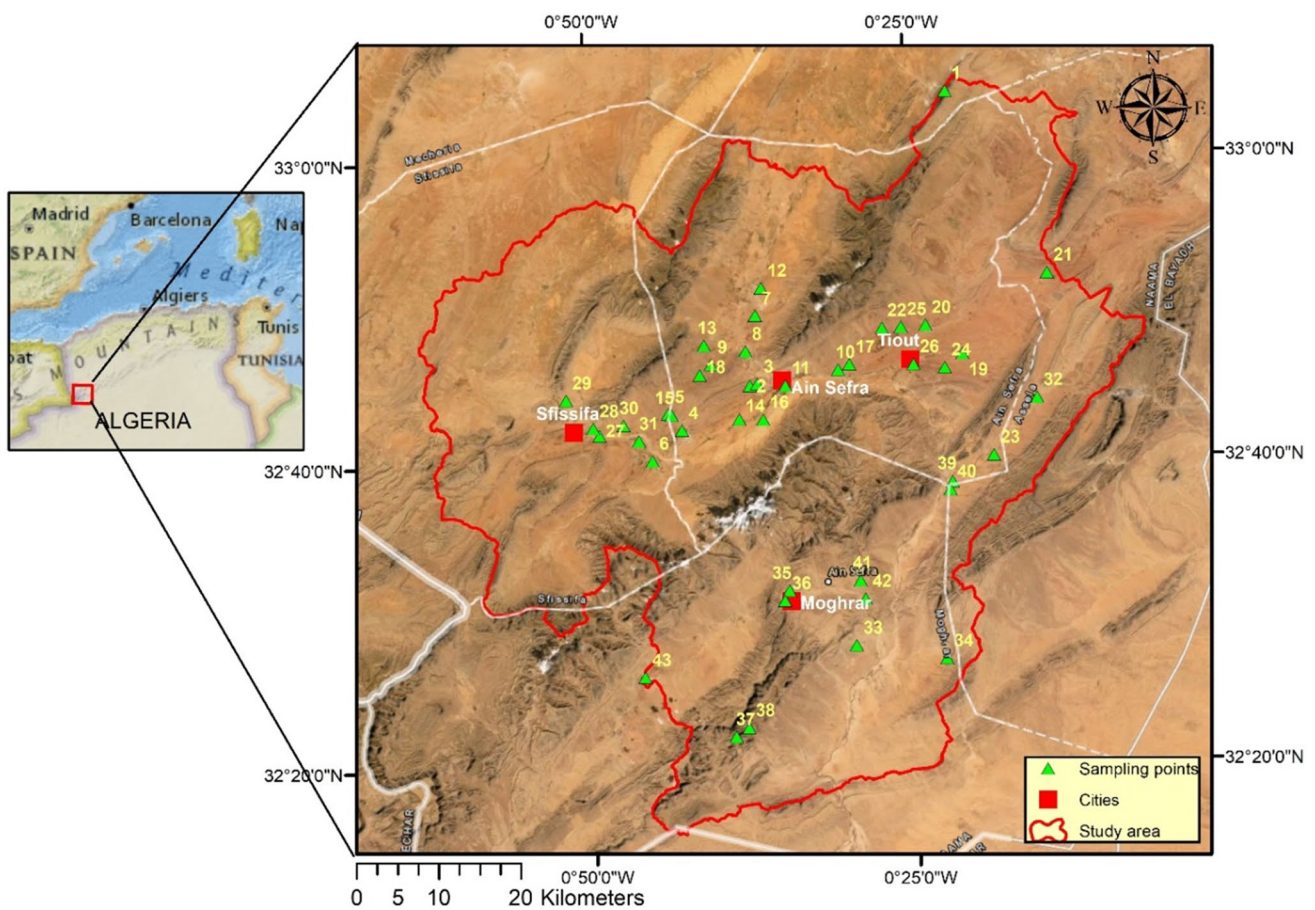
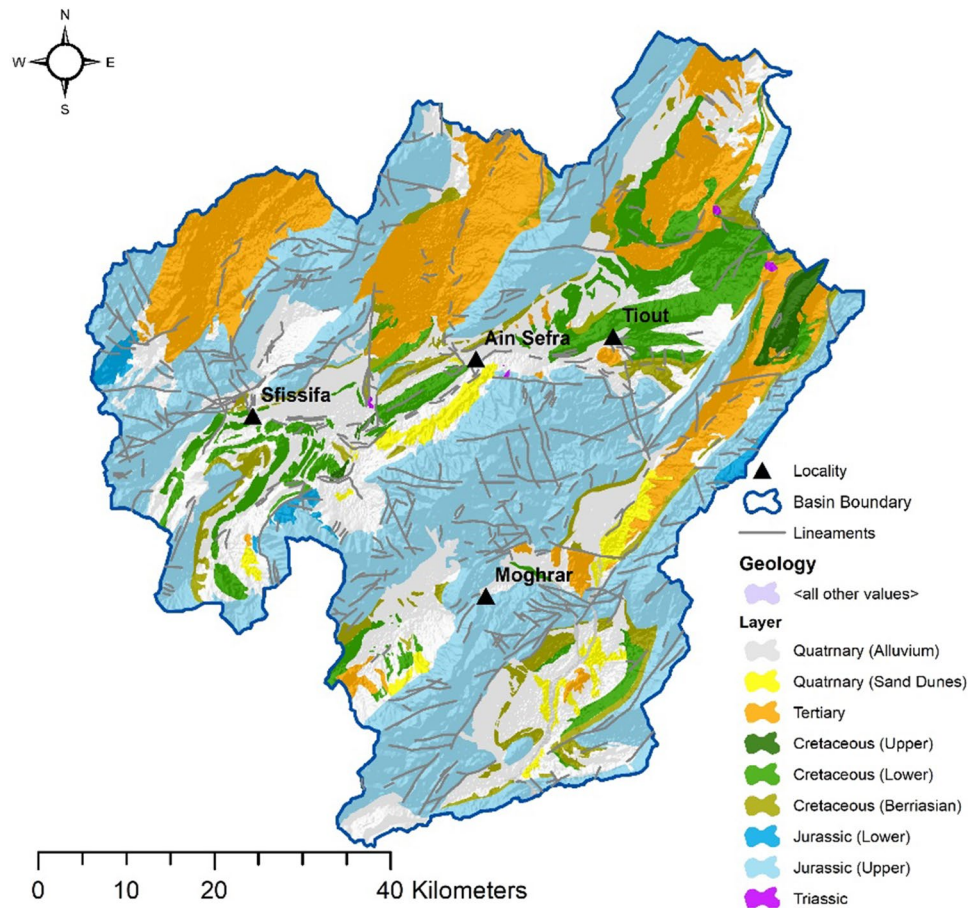


Fig. 1 Study area: the Ain Sefra watershed

**Fig. 2** Geologic Map of the Ain Sefra watershed (Derdour et al. 2022)



Most of the outcrops belong to the Mesozoic formations in the Ksour Mountains. The Cenozoic sediments of the Atlas are in depressions and are represented by the continental Tertiary discordant in the small fragmented secondary. In the Southern Saharian Atlas, the post-Turonian formations are more continuously observed (Rahmani et al. 2017). The Triassic comprises versicoloured clays with gypsum and salt, while the Jurassic comprises sandstones and clays. The Berrasian or Tiloula Formation is greenish and white sandstones with gypsum clays siltstones. Barremian and Albian (“Tiout formation”) have a thickness of about 1065 m. The sandstones exist in extensive areas, occupying the heart of the synclines of the Western Sahara Atlas. This formation is divided into lower, middle, and upper members. The Cenomanian–Turonian comprises an assemblage of greenish-grey gypsiferous pelitic clays, massive dolomitic limestones, and whitish marls. The Tertiary continental series is attributed to the Mio-Pliocene and comprises scattered red sandstone layers with gypsiferous formations. The Quaternary comprises dunes and alluvial formations, located especially in the Wadis above the basin (Rahmani et al. 2017). From a hydrogeological standpoint, the watershed has three groundwater resources aquifer systems: the Quaternary aquifer, the lower Cretaceous sandstone aquifer

and the Jurassic sandstone aquifer (Rahmani et al. 2017). The Albian aquifer is the largest groundwater reservoir in the research area, comprising altered sandstones and clays at the bottom and sandstones at the top (Rahmani et al. 2017). Pores and cracks characterise of this confined aquifer. In the Ain Sefra region, part of the Mont des Ksour, agriculture has broadened in recent years, which has led decision-makers to develop geophysical and hydrogeological studies to exploit the region’s groundwater.

Consequently, a series of boreholes were drilled along the syncline, exploiting over 100,000 m<sup>3</sup>/day. Ain Sefra watershed comprises a set of synclines in which Cretaceous and Jurassic sandstones represent most layers. It is enclosed between Aissa, Morghad, and Bouamoud in the North and the anticlines of Mekther, Mir El Djbel, and Mzi in the South (Derdour et al. 2018). The study area comprises four soil groups: mineral soils, saline soils, limestone-magnetic soils, and graded soils (Bouarfa and Bellal 2018). It is characterised by two major seasons, a cold one with the smallest temperatures that can reach 0 °C, and a warm one marked by the greatest temperatures of 36 °C. It belongs to the arid to the semi-arid climatic stage, in which rainfall is infrequent but violent, and evaporation is significant (Melalih and Mazour 2021). Annual precipitation ranges from 135

to 280 mm, with an average of 195.6 mm per year (Derdour et al. 2018).

### Data acquisition

Groundwater quality data were collected in March 2022 from forty-three (43) boreholes to assess the aquifer system underlying the study area (Fig. 2). Samples were distributed to cover most of the study area. All water samples were gathered in polypropylene (PP) bottles that had been rinsed several times with sample water before collection and then stored at 04 °C in the field. Afterwards, all water samples were transferred to Naâma university laboratory for analysis. The samples were analysed the day they were collected. A portable multi-parameter type HANNA (HI98194) was used to measure in situ: temperature, total dissolved solids (TDS; which refer to the total amount of dissolved substances in a volume of water), the potential of hydrogen (pH), and electrical conductivity (EC). Bicarbonates were measured by titration, while nitrate (NO<sub>3</sub><sup>-</sup>) and sulphates (SO<sub>4</sub><sup>-2</sup>) were determined with a UV–VIS spectrophotometer. Sodium (Na<sup>+</sup>) and potassium (K<sup>+</sup>) were assessed using a flame photometer. The complex metric titration method was used to find the total hardness (TH), calcium (Ca<sup>++</sup>), and magnesium (Mg<sup>++</sup>). Chloride (Cl<sup>-</sup>) concentrations were identified using Mohr’s technique.

### Gibbs diagram

The Gibbs diagram is a popular method for analysing the relationship between water composition and lithological properties of aquifers. The Gibbs diagram depicts three distinct domains: rock-water interaction, evaporation, and precipitation (Gibbs 1970). Scatter plots were plotted in a Gibbs diagram with (Na<sup>+</sup> + K<sup>+</sup>)/(Na<sup>+</sup> + K<sup>+</sup> + Ca<sup>++</sup>) and (Cl<sup>-</sup>)/(Cl<sup>-</sup> + HCO<sub>3</sub><sup>-</sup>) as the abscissa and Total Dissolved Solids (TDS) as the ordinate. The Gibbs ratios are computed from the following equations (Eqs. 1, 2):

$$\text{Ration for cations} = \frac{(Na^+ + K^+)}{(Na^+ + K^+ + Ca^{++})} \tag{1}$$

$$\text{Ration for anions} = \frac{Cl^-}{(Cl^- + HCO_3^-)} \tag{2}$$

It should be noted that all ionic concentrations are represented in meq/l (Gibbs 1970).

### Piper plot

The Piper plot or diagram was used to understand issues related to groundwater geochemical dynamics. The Piper

diagram was used to classify the diverse groundwater facies (Piper 1944). There are three separate fields in this diagram, including a diamond-shaped field and two triangular areas. Cations are plotted as a single point in the left triangle in proportion to total cations in meq/l, because anions are placed in the other triangle. Each parameter is then projected into the upper field along a parallel line. The intersection of this parallel with the upper edge characterises the water, as shown by the interaction between cations and anions. The trilinear diagram can show similarities and variations among groundwater samples. Based on this diagram, samples of comparable quality will be presented together as groups.

### Water quality index (WQI)

The “WQI” indicator shows the overall quality of water fit for human consumption considering the effects of much water quality criteria (Brown et al. 1972; Chakraborty et al. 2021; Horton et al. 1965). The WQI is calculated:

–Step 01: Allocating a weight (Wi). In this step, a weight (wi) has been assigned to each of the 12 physicochemical limits of the study (Table 1). This weight reflects the relative importance in terms of overall drinking water quality.

Nitrates and TDS were assigned the largest weighting rate of 5 because of their important influence on groundwater quality. Magnesium had the lowest weighting rate (1) because of its low influence in determining water quality. Other factors (pH, EC, Na<sup>+</sup>, Ca<sup>++</sup>, Cl<sup>-</sup>, SO<sub>4</sub><sup>-2</sup> and TH) were assigned to values between 2 and 4 according to their significance in assessing water quality (Damo et al. 2013; Nong et al. 2020), as shown in Table 1.

**Table 1** Weighting of each physicochemical parameter

PC-parameters	Units	Algerian Standard (AS)	Weight (wi)	Relative weight (Wi)
pH		8.5	4	0.108
Electrical Conductivity	µS cm <sup>-1</sup>	2800	4	0.108
TDS	mg l <sup>-1</sup>	1500	5	0.135
Magnesium (Mg <sup>++</sup> )	mg l <sup>-1</sup>	50	1	0.027
Calcium (Ca <sup>++</sup> )	mg l <sup>-1</sup>	200	2	0.054
Potassium (K <sup>+</sup> )	mg l <sup>-1</sup>	12	2	0.054
Sodium (Na <sup>+</sup> )	mg l <sup>-1</sup>	200	2	0.054
Chlorides (Cl <sup>-</sup> )	mg l <sup>-1</sup>	500	3	0.081
Sulphates (SO <sub>4</sub> <sup>-2</sup> )	mg l <sup>-1</sup>	400	4	0.108
Nitrates (NO <sub>3</sub> <sup>-</sup> )	mg l <sup>-1</sup>	50	5	0.135
Bicarbonates (HCO <sub>3</sub> <sup>-</sup> )	mg l <sup>-1</sup>	120	3	0.081
TH	mg l <sup>-1</sup>	200	2	0.054
			37	1

–Step 02 Proportional weight calculation. Equation 3 was used to compute the proportionate weight ( $W_i$ ) in this step:

$$W_i = w_i / \sum_{i=1}^n w_i \quad (3)$$

where  $W_i$  denotes the proportional weight,  $n$  is the total number of parameters, and  $w_i$  denotes the weight of each parameter (Brown et al. 1972).

–Step 03 Rating scale of quality assignment. Then, Eq. 4 was used to set up the quality rating scale ( $q_i$ ) for each parameter:

$$q_i = (C_i/S_i) \times 100 \quad (4)$$

where  $q_i$  denotes the quality rating scale,  $C_i$  denotes the concentration of each chemical parameter in  $\text{mg.l}^{-1}$  and  $S_i$  denotes the drinking water standards ( $\text{mg l}^{-1}$ ) (third column in Table 1).

–Step 04 Sub-index value determination. The sub-index values  $SI_i$  for all chemical characteristics are determined in this phase by multiplying the proportional weight, as shown in Eq. 5 (Chakraborty et al. 2021; Horton and Hawkins 1965):

$$SI_i = W_i \times q_i \quad (5)$$

–Step 05 Final WQI calculation. WQI was calculated in the last phase by summing all the sub-indices from all samples of the study area together, as described in Eq. 6:

$$WQI = \sum SI_i \quad (6)$$

where  $SI_i$ ,  $i$  is the parameter's subindex (Brown et al. 1972; Horton and Hawkins 1965).

–Step 06 WQI classification. Thus, the results of the computed Water Quality Index (WQI) were divided into five groups: (i) if the WQI is greater than 300, the water is unsafe to drink; (ii) when the WQI is between 200 and 300, the water is very poor; (iii) in the case of WQI, it ranges between 100 and 200, the water is poor; (iv) when the WQI is between 50 and 100, the water is good; and v) if the WQI is less than 50, the water is excellent.

## Spatial variation

The study area boundaries were digitised using the ArcGIS software (ArcGIS 2020). Using a GARMIN-GPS Forerunner-945, the precise locations of monitoring water points were well-recorded.

The Inverse Distance Weighted (IDW) interpolation method (Shepard 1968; Charizopoulos et al. 2018) was used to analyse the spatial variation of a pollutant load and nutrient concentrations ( $\text{mg l}^{-1}$ ). With this approach,

spatial variation maps were generated (Achilleos 2011; Maleika 2020). The IDW has employed a deterministic model method, which calculates unknown values based on the closeness of adjacent points (Asadollah et al. 2023). This IDW approach is used to characterise pollutant distribution and to find physicochemical patterns in space and time (Kanagaraj and Elango 2016). Spatial distribution maps of EC, TH, pH, TDS, major cations, major anions, and WQI were generated for the Ain Sefra catchment. These maps can be useful tools for decision-making and water resource management.

## Pearson correlation

Pearson's correlation coefficient was calculated with the WQI and other water quality limits. This coefficient underlines how much each parameter matters and its effect on the hydrochemical process in the case of the Ain Sefra watershed. If (R) values of the Pearson's correlation matrix are close to +1 or –1, they are strong correlation coefficients and represent total correlation, or functional dependence, between two variables (Asadollah et al. 2023; de Vente et al. 2011). If the values are close to zero, no significant interaction exists between the two variables. The parameters are highly correlated if R is greater than 0.8 and are moderately correlated if R is between 0.4 and 0.8 (Tajmunnaher et al. 2017).

The general flowchart of the procedure that visualizes this approach's stages is shown in Fig. 3, where Step 1 informs that the data were gathered during March 2022 following the USGS normal procedures, as described in “Data acquisition”. These data were required to do spatial interpolations. In Step 2 data, gathered in step 1, were used to calculate the Water Quality Index (WQI), as described in “Water Quality Index (WQI)”. In Step 3, the Gibbs and Piper diagrams were performed in “Gibbs diagram” and “Piper plot”. Finally, in Step 4, correlation analysis was accomplished to highlight the relevance of each parameter independently and their effect on the hydro chemistry process in the Ain Sefra basin.

## Results and discussion

### Characterisation of the groundwater samples

Table 2 shows the data collected from the study catchment, where physicochemical parameters and hydrochemical properties were calculated. Key values of these parameters are shown within four statistical analyses: the minimum (Min), the maximum (Max), the mean and the standard deviation (SD). Detailed information on these parameters can be found

Fig. 3 Workflow of the system

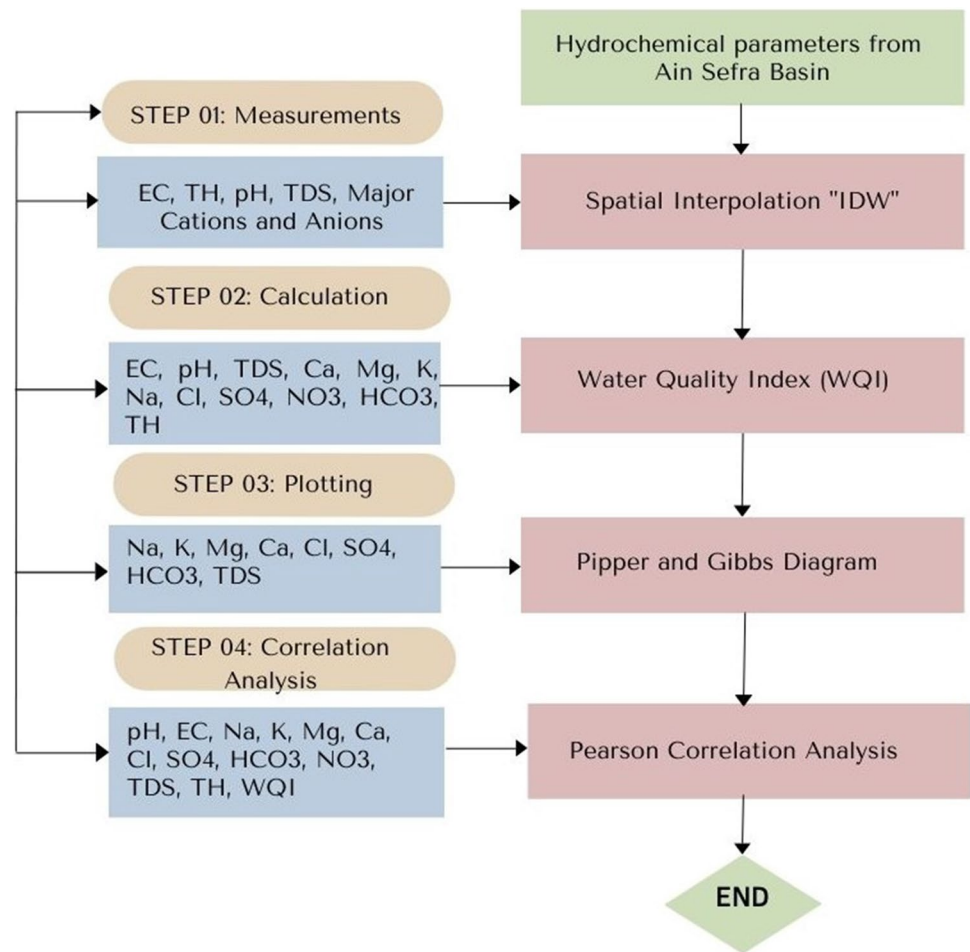


Table 2 Data of groundwater quality parameters of the Ain Sefra watershed

Parameters	Min	Max	Mean	SD
pH	7.03	8.5	7.75	0.43
EC ( $\mu\delta\text{ cm}^{-1}$ )	200	5500	1265.12	946.13
TDS ( $\text{mg l}^{-1}$ )	339	3220	1089.02	683.91
$\text{NO}_3$ ( $\text{mg l}^{-1}$ )	1	97	26.51	21.02
$\text{SO}_4^{-2}$ ( $\text{mg l}^{-1}$ )	38	1512	305.28	298.44
Cl ( $\text{mg l}^{-1}$ )	10	631	181.28	147.74
$\text{HCO}_3$ ( $\text{mg l}^{-1}$ )	141	360	232.28	46.77
TH	16.28	156.31	55.72	29.11
Ca ( $\text{mg l}^{-1}$ )	12	427	130.65	78.73
Mg ( $\text{mg l}^{-1}$ )	5	160	56.21	29.64
Na ( $\text{mg l}^{-1}$ )	5	390	107.29	96.08
K ( $\text{mg l}^{-1}$ )	2	31	7.71	5.38

in the Supplementary material of the present manuscript. Likewise, these results were compared with Algerian standards (JORADP 2011).

### Spatial distribution of the physico-chemical parameters

The Inverse Distance Weighted (IDW) interpolation approach has been used to create various spatial distribution maps of physicochemical parameters. This interpolation method showed the best model performance among the considered methods (Table 3).

The highest pH and TDS values are found in the Tiout region (Fig. 4a, b). The electrical conductivity (EC) measurements were successful (except in well number (33)), because the measured values were below the limit for water set by the standards ( $2800\ \mu\delta\text{ cm}^{-1}$ ; Fig. 4c). The lowest mean value (of  $200.0\ \mu\delta\text{ cm}^{-1}$ ) was found at borehole number 35. Therefore, a close relationship between electrical conductivity (EC) and TDS has been identified. In this current research work, the observed total hardness range was  $16.28\text{--}156.31\ \text{mg l}^{-1}$ , where total hardness (TH) values show a gradual increase from west to east (Fig. 4d).

In accordance with the spatial distribution of calcium (Fig. 5a), only three wells (No.13, No.19, and No.21) exceed

**Table 3** Performance of eleven interpolation methods in the Ain Sefra watershed considering the Pearson correlation (R) and the Root Mean Square Error (RMSE)

Interpolation method	Statistical contrasts	
	R	RMSE
Inverse distance weighting	0.67	17.19
Global polynomial interpolation	-0.17	22.81
Radial basis functions	-0.33	19.12
Local polynomial interpolation	0.53	20.98
Ordinary Kriging	0.12	20.64
Simple Kriging	-0.35	20.89
Universal Kriging	0.12	20.64
Areal interpolation	-0.55	24.28
Empirical Bayesian Kriging	0.13	18.63
Kernel smoothing	-0.34	19.61
Diffusion kernel	-0.42	26.71

the Algerian standards. In the spatial distribution of magnesium (Fig. 5b), it can be observed that the Tiout region depicts a high concentration of magnesium. It should be noted that magnesium has a lower concentration than calcium. Spatial analysis of potassium at the water sampling points showed that most of the samples had potassium concentrations within the desired range of  $12 \text{ mg l}^{-1}$  (Fig. 5c). Figure 5d shows the spatial distribution of sodium. The highest concentrations of sodium ( $360 \text{ mg l}^{-1}$  and  $390 \text{ mg l}^{-1}$ ) have been found in the groundwater samples (No.32 and No.24).

Based on to the spatial analysis of chloride, the highest chloride concentration is found in the Southwestern part of the research area (Fig. 6a). In the spatial distribution of bicarbonates (Fig. 6b), it can be observed that the south of the study area depicts a high concentration of bicarbonates. The lowest values of nitrate concentration were detected in the southern part of the study area (Fig. 6c). In addition, a gradual increase is observed from the south to the north, justified by agricultural activity in this area. Significant levels of sulphates in groundwater samples are presented in well number 13 as reported by the spatial analysis of sulphates in the study area (Fig. 6d).

### Piper plot

Grapher software (Version 16.2.354) has been used to plot the geochemical results on a Piper trilinear plot (Fig. 7). The groundwater collected in the Ain Sefra basin has shown that mixed Ca-Mg-SO<sub>4</sub>-Cl facies predominate. Most of the samples in our study belong to the mixed Ca-Mg-SO<sub>4</sub>-Cl zone. This results in the chemical masking of the groundwater because of rock-water interaction, longer residence time, and reactions within the unsaturated zones.

### Gibbs plot

The Gibbs plot depicted that the predominant samples fall in the dominant rock-water interaction field of this diagram and, to this extent, in the evaporation domain (Fig. 8). The dominant rock-water interaction field shows how rock chemistry interacts with the chemistry of penetrable subsurface water (Boansi-Okofe et al. 2021; El Osta et al. 2022).

Thus, water-rock interaction is the crucial factor controlling the chemical composition of groundwater. The results showed that the chemical compositions of water depend on the geology, where the groundwater is located. Thus, salinity affects the groundwater in the Berrassian formations characterised by evaporite minerals. The saline contamination occurred during the groundwater recharge period. In the case study, a better quality of groundwater samples was observed in the Albian formations.

### Water quality index (WQI) assessment

Using the inverse distance weighted (IDW) approach, the map of the spatial distribution of the “WQI” for groundwater samples was created for the Ain Sefra watershed (Fig. 9). Table 4 shows the WQI calculation for the groundwater samples. It has been concluded that in 9 samples falling into the excellent category, 30 were classed as good. The WQI in three wells in the area (13, 19, 24 and 26) was characterised as poor because of high electrical conductivity values, total dissolved solids, and sulphate concentration. According to our findings, the best groundwater samples are found in Cretaceous (Upper and Albian) formations, which confirms the results of the Gibbs plot. In contrast, the wells close to the poor water are in Berrassian formations (“Tiloula”). From this, we deduce that the water quality deterioration was related to the geological formations. Mineralized water is leached with chemical elements during the groundwater recharge period.

The main evaporite minerals gypsum, anhydrite, halite; and halite-related evaporite minerals, such as epsomite, bischofite, and sylvite dissolve in water and enrich it with sulphates and chlorates. Consequently, the WQI map of the study area is a valuable and effective tool for disseminating and monitoring data to decision-makers. In this way, a better overview of the current groundwater quality in the region is achieved.

### Correlation analysis

This study examines the correlation between chemical parameters and WQI values using a correlation matrix (Table 5). It is observed that potential hydrogen (pH), nitrate (NO<sub>3</sub><sup>-</sup>) and bicarbonates (HCO<sub>3</sub><sup>-</sup>) are not correlated with other variables. Pearson’s coefficient ranges from -0.311



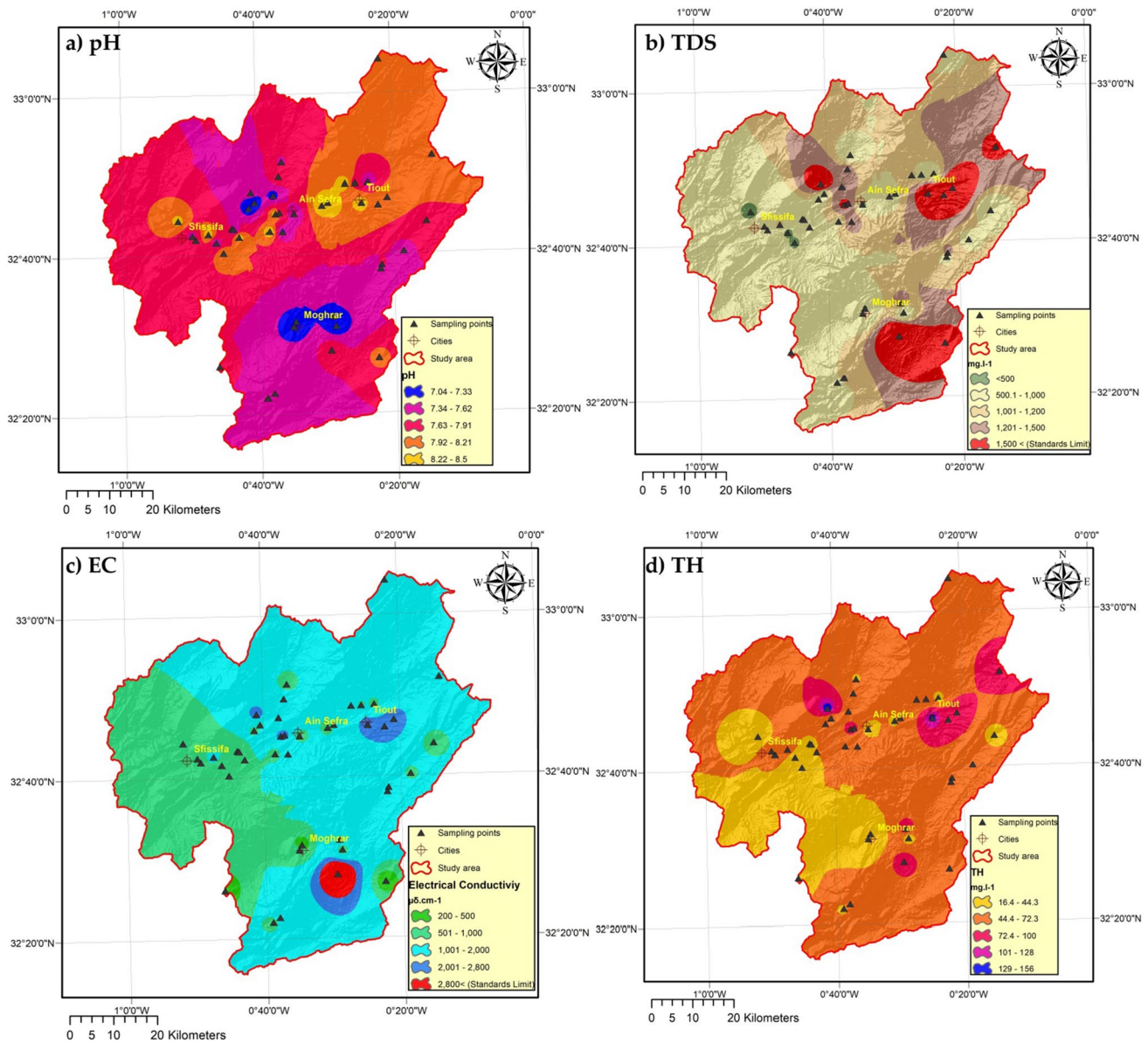


**Fig. 4** Spatial distribution of the Ain Sefra watershed **a** pH, **b** TDS, **c** EC, **d** TH

and 0.282;  $-0.276$  and  $0.1$  and  $-0.072$  and  $0.102$ , respectively. Total hardness (TH), Total Dissolved Solids (TDS) and sulphates ( $SO_4^{2-}$ ), are significantly correlated, reflecting a correlation value higher than 0.80.

The WQI shows low correlations with a potential hydrogen (pH), nitrates ( $NO_3^-$ ) and bicarbonates ( $HCO_3^-$ ). It shows moderate correlations with chlorides ( $Cl^-$ ), sodium ( $Na^+$ ), and potassium ( $K^+$ ), and finally, excellent correlations with total dissolved solids (TDS), electrical conductivity (EC), total hardness (TH), sulphates ( $SO_4^{2-}$ ), calcium ( $Ca^{++}$ ) and magnesium ( $Mg^{++}$ ). The greater influence on groundwater quality of these chemical parameters confirms that the

chemical compositions of water depend (to a large extent) on the geology, where the groundwater is located.

**Discussion**

Much information has been achieved in the groundwater gathered in the Ain Sefra basin, which was tested within Algerian Standards (JORADP 2011). The potential of hydrogen (pH) depicted ranges between 7.03 and 8.50 and its average is 7.75 (alkaline region as  $pH > 7.0$ ). These findings are similar to the results of the study of Derdour et al. (2020) in the Naâma watershed, located approximately 70 km north of the Ain Sefra basin, where they reported a mean pH of 7.71.

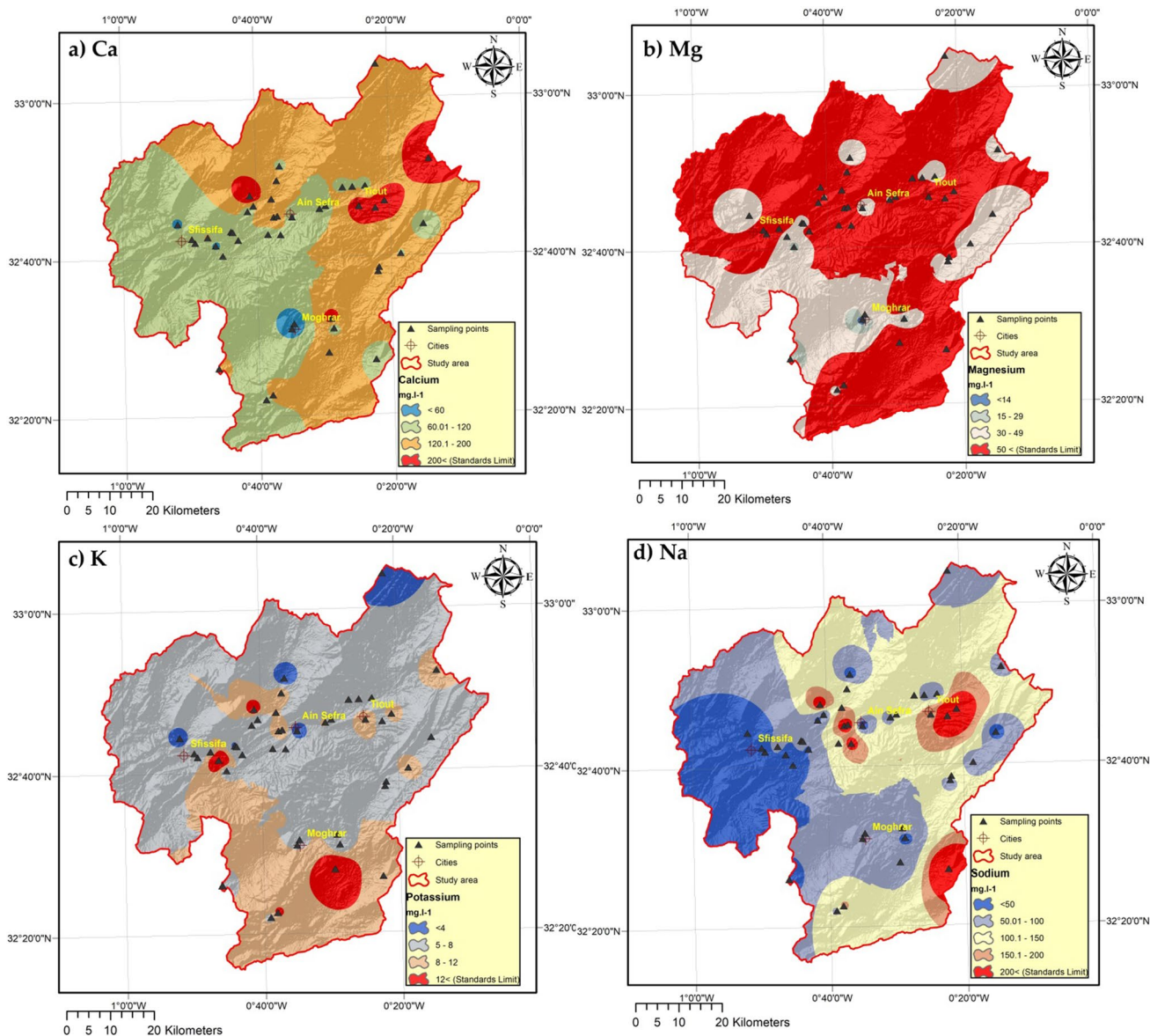


**Fig. 5** Spatial distribution of major cations in the Ain Sefra watershed: **a**  $\text{Ca}^{++}$ , **b**  $\text{Mg}^{++}$ , **c**  $\text{K}^{+}$ , **d**  $\text{Na}^{+}$

The TDS concentrations in the samples from our research area vary from 339 to 3220  $\text{mg.l}^{-1}$ . WHO recommendations specify a limit of 1000  $\text{mg.l}^{-1}$  (WHO 2011) and this limit is met in 65% of the water samples. It should be noted that Algerian standards do not stipulate a limit for TDS (JORADP 2011). The values achieved are adequate in 42 of the 43 boreholes analysed (TDS values below 3000  $\text{mg.l}^{-1}$ ) (Sarath-Prasanth et al. 2012). Boreholes 33 and 13 showed high values (3220 and 2886.4  $\text{mg.l}^{-1}$ ; Table 2) to be analysed. These results are lower than those reported in the study of Hamlat and Guidoum (2018), which assessed groundwater quality in six major urban centers in Northwestern Algeria (Oran, Ain Témouchent, Tlemcen, Sidi Bel Abbes, Saida, and Mascara), where TDS levels varied from 400 to

6400 ppm. In cities like Baghdad, values exceeding 600 ppm were found (Al-Dulaimi and Younes 2017), the greatest permissible value for drinking water. The EC of the samples in the research area ranges from 200.0 to 5500.0 ( $\mu\text{S cm}^{-1}$ ), with a mean value of 1265.12 ( $\mu\text{S cm}^{-1}$ ). These values significantly surpass the EC levels found in the Naama watershed, where electrical conductivity ranged from 551 to 1084  $\mu\text{S/cm}$ , with an average value of 777.14  $\mu\text{S/cm}$ . Moreover, our results also exhibit considerably higher EC values compared to other countries' findings, such as Guinea-Bissau with 521  $\mu\text{S/cm}$  (Bancesi et al. 2020), Ethiopia with 192.14  $\mu\text{S/cm}$  (Meride and Ayenew 2016), and 170.6  $\mu\text{S/cm}$  (Desye et al. 2021).

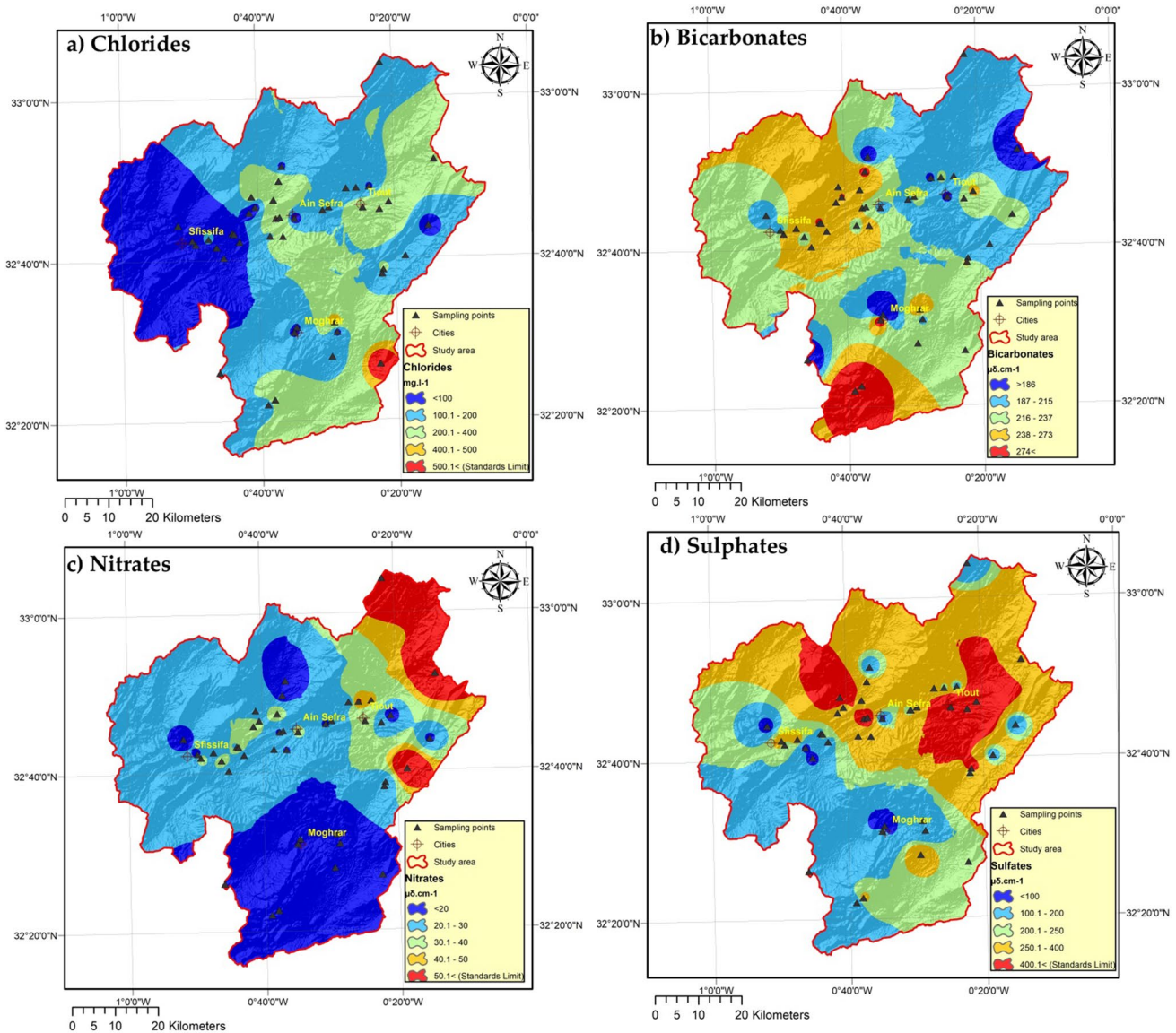


**Fig. 6** Spatial distribution of major cations in the Ain Sefra watershed: **a** chlorides; **b** bicarbonates; **c** nitrates; **d** sulphates

Calcium concentrations in the research’s groundwater area range from 12 to 427 mg.l<sup>-1</sup>, significantly higher than those observed in the Adrar region located in the south of Algeria, in the study conducted by Bendida et al. (2021), where the mean calcium concentration was reported as 87.82 mg l<sup>-1</sup>. Furthermore, the calcium values in our study surpass those found in Taiwan, where Yang (1998) reported 34.7 mg l<sup>-1</sup>, as well as in the US and Canada (Morr et al. 2006), where values ranged between 1 and 135 mg l<sup>-1</sup>, with an average of 21.8 mg l<sup>-1</sup>. Although most of the calcium concentrations in our research fall within the permissible range defined by the Algeria’s standards, which set a maximum value of 200 mg l<sup>-1</sup>, there are notable differences compared to other regions and countries (JORADP 2011).

Magnesium values found in the research area ranges from 5.0 mg l<sup>-1</sup> to 160.0 mg l<sup>-1</sup>. These values are somewhat similar to the results observed in the Saida aquifer system, located in the western part of Algeria, where magnesium concentrations ranged from 12.2 to 148.8 mg l<sup>-1</sup> (Djidi et al. 2008). Other works identified values of 13.5 mg l<sup>-1</sup> of magnesium in Taiwan (Yang 1998), as did a study focused on identifying relationships between Ca and Mg concentrations in drinking water and the risk of cardiovascular disease (Nerbrand et al. 2003). Other approaches in Slovakia identified values of 78–155 mg l<sup>-1</sup> and 28–54 mg l<sup>-1</sup> for calcium and magnesium as adequate for reducing mortality in cardiovascular diseases (Rapant et al. 2017). In the Ain Sefra basin, the magnesium results (except well number 15) are within standard limits (around 150 mg l<sup>-1</sup>).

**Fig. 7** Piper trilinear diagram in the Ain Sefra basin

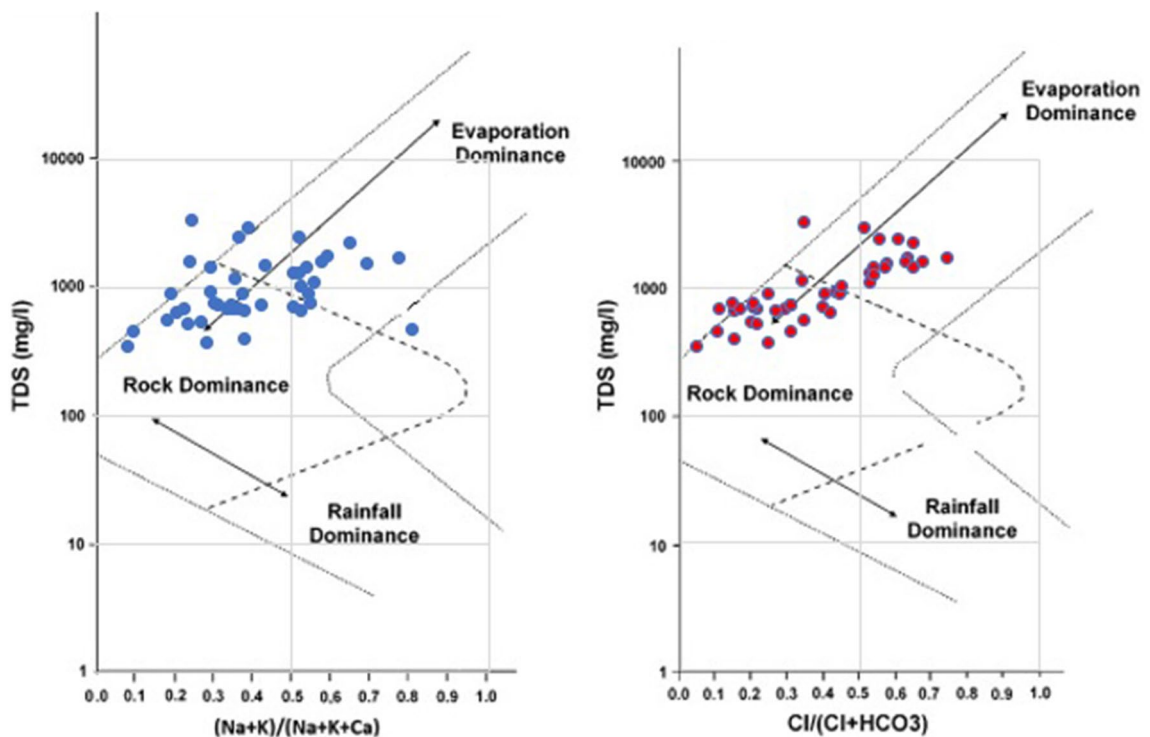
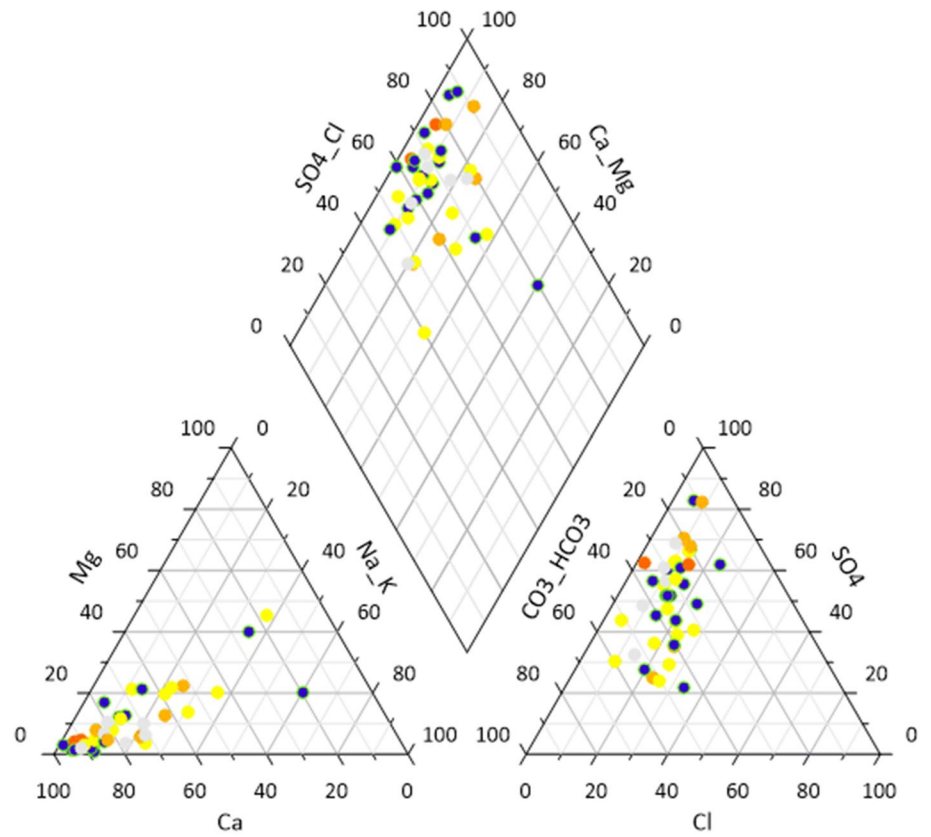


**Fig. 8** Gibbs diagram of the Ain Sefra basin

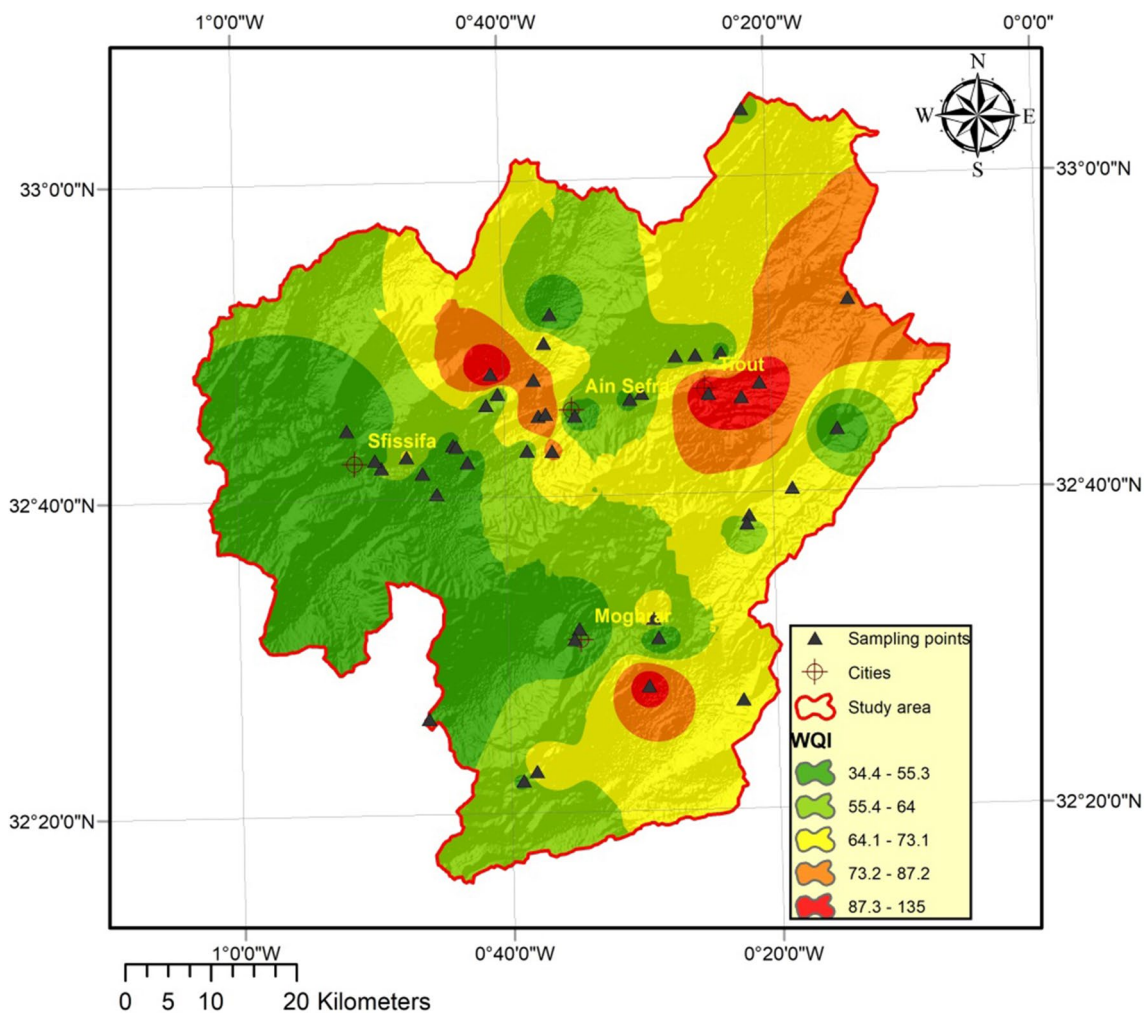


Fig. 9 Spatial distribution of WQI in the Ain Sefra watershed

The sodium values in the water sampling points in our study area are found to be between 21 and 390 mg l<sup>-1</sup> (the greatest concentration allowed in drinking water, 200 mg l<sup>-1</sup>). These values are lower than the sodium levels reported in the Naama watershed study conducted by Derdour et al. (2020), where sodium ranged from 21 to 806 mg l<sup>-1</sup>. Similar values (below 200 mg l<sup>-1</sup>) were found in Ethiopia (Arega 2020). Drinking water is a source of daily sodium and a risk factor for hypertension. Some approaches quantified 20% of stroke death are because of high-sodium diets (Scheelbeek et al. 2017) and each 100 mg l<sup>-1</sup> reduction in sodium in drinking water involved a blood pressure reduction of 0.95 and 0.57 mmHg in systolic and diastolic blood pressure (IHME 2015). The average potassium concentration ranges from 2 mg l<sup>-1</sup> in well number 12 to 31.23 mg l<sup>-1</sup> in well number 31. Similar values to these recognized were reached in Adrar, Algeria: 7–29.6 mg l<sup>-1</sup> (Bendida et al. 2021), Malaysia: 0–36.7 mg l<sup>-1</sup> (Hamzah et al. 2014). Average concentrations of potassium in raw

drinking water vary between 1 and 8 mg l<sup>-1</sup> (Canada 2008). The mean cations concentration followed a descending order as Ca<sup>++</sup> > Na<sup>+</sup> > Mg<sup>++</sup> > K<sup>+</sup>, being their concentrations 130.7, 107.3, 56.2, and 7.6 mg l<sup>-1</sup>, respectively.

The mean chloride values in this study area ranged from 10 mg l<sup>-1</sup> in groundwater sample number 11 to 631 mg l<sup>-1</sup> in groundwater sample number 34. Except for sample number 34, the chloride concentration was within the guideline range established by Algerian Standards. Comparatively, the chloride levels in our study are lower than those found in the western region of Algeria, as reported by Hamlat and Guidoum (2018), where chloride concentrations ranged between 370 and 3618 mg l<sup>-1</sup>. The presence of high chloride, sodium, and EC levels, along with elevated calcium, strongly suggests that rock-water interactions play a significant role in deteriorating groundwater quality.

Bicarbonate concentrations range from 141 to 360 mg per litre. These values are higher compared to the bicarbonate levels found in the Naama watershed, where they ranged

**Table 4** Classification of each sample using the Water Quality Index (WQI)

S. No	WQI value	Water quality classification	S. No.	WQI value	Water quality classification
No 1	73.45	Good	No 23	80.97	Good
No 2	98.13	Good	No 24	115.53	Poor
No 3	97.47	Good	No 25	68.80	Good
No 4	59.19	Good	No 26	132.46	Poor
No 5	58.93	Good	No 27	65.66	Good
No 6	49.39	Excellent	No 28	59.34	Good
No 7	81.54	Good	No 29	40.93	Excellent
No 8	88.87	Good	No 30	76.71	Good
No 9	60.74	Good	No 31	61.15	Good
No 10	57.99	Good	No 32	49.70	Excellent
No 11	44.39	Excellent	No 33	114.72	Good
No 12	41.26	Excellent	No 34	82.46	Good
No 13	154.40	Poor	No 35	49.01	Excellent
No 14	66.65	Good	No 36	56.60	Excellent
No 15	67.91	Good	No 37	60.03	Good
No 16	88.08	Good	No 38	83.50	Good
No 17	71.32	Good	No 39	86.12	Good
No 18	63.64	Good	No 40	61.39	Good
No 19	118.79	Poor	No 41	84.01	Good
No 20	57.80	Good	No 42	47.38	Excellent
No 21	98.04	Good	No 43	43.29	Excellent
No 22	69.94	Good			

from 190 to 272 mg l<sup>-1</sup> (Derdour et al. 2020). When nitrate concentrations exceed 100 mg l<sup>-1</sup>, they become detrimental to certain aquatic species. The nitrate concentration in the study's groundwater ranges from 1.02 mg.l<sup>-1</sup> at sampling station No.36 to 97.3 mg l<sup>-1</sup> at sampling station No.23, with a mean value of 26.51 mg l<sup>-1</sup>. These values closely resemble the results reported in other regions: Adrar with 23.97 mg l<sup>-1</sup> (Bendida et al. 2021), Naama with 28.6 mg l<sup>-1</sup> (Derdour et al. 2020) and Bechar with 28 mg l<sup>-1</sup> (Kendouci et al. 2019). Approximately 94% of the groundwater was within the Algerian Standards (50 mg l<sup>-1</sup>). The mean sulphates concentration ranges between 38.0 and 1512.0 mg l<sup>-1</sup> in the groundwater samples. Some observe that the guide value (400 mg l<sup>-1</sup>) prescribed by Algerian Standards (2011) is met for all samples, except for No.14, No.19, No.24, No.26 and No.39. These sulfate values are significantly higher than those obtained in the study conducted by Mansouri et al. (2022) in the Ouargla Basin, placed in the South of Algeria, where sulfate values ranged from 476.00 to 2290 mg l<sup>-1</sup>. For anions, the mean concentration follows a descending order as SO<sub>4</sub><sup>-2</sup> > HCO<sub>3</sub><sup>-</sup> > Cl<sup>-</sup> > NO<sub>3</sub><sup>-</sup>, being their concentrations 305.3, 232.3, 181.3, and 26.5 mg l<sup>-1</sup>, respectively.

The Water Quality Index, Gibbs and Pipers plots and correlation analysis were used to show whether the water samples from the Ain Sefra watershed are safe for human use. From a health standpoint, excessive levels of calcium and magnesium in tap water from the studied area are not harmful to human health. Nevertheless, they may alter the taste of the water. The groundwater samples from the study area belong to the soft water category (TH > 150 mg l<sup>-1</sup>). There are no obvious health effects of high conductivity. Potassium and sodium are necessary elements for humans but are rarely, if ever, found in drinking water in amounts harmful to healthy people. High sulphate values in drinking water involve a detectable taste, and if the amount is high, it can have a laxative effect on people who are not used to it. High sulphate values are distributed in the regions of the Berrassian formations that are characterised by evaporite minerals. The highest chloride concentration is found towards the south, which gives a saline taste and may cause laxative effects on unaccustomed people.

Results showed that cations were in the following order: Ca<sup>++</sup> > Na<sup>+</sup> > Mg<sup>++</sup> > K<sup>+</sup> and anion abundance was in this order: SO<sub>4</sub><sup>-2</sup> > HCO<sub>3</sub><sup>-</sup> > Cl<sup>-</sup> > NO<sub>3</sub><sup>-</sup>. Thus, compared to many approaches listed above, such as Rao and Nageswararao (2013), Sadat-Noori et al. (2014), Nong et al. (2020), Derdour et al. (2020) and Derdour et al. (2021), the methods used offer better results, which can be extrapolated to many arid areas. In the present study, our results showed that the chemical compositions of water depend on the geology, where the groundwater is located. Similar trustworthy findings were achieved by Derdour et al. ((2020), Boansi-Okofu et al. (2021), Latha (2022), El Osta et al. (2022), Hornero-Díaz (2018), Pla et al. (2021) and Baudron (2013) in arid areas of Argelia, Ghana, Saudi Arabia, India and the south-east of Spain.

## Conclusions

The main conclusions obtained in the present study are listed here:

- (i) Most of the water quality measurements tested in the Ain Sefra basin, together with pH, EC, major anions and cations and TDS, were within the limits allowed by Algerian standards. The principal anion and cation abundances are in descending order: SO<sub>4</sub><sup>-2</sup> > HCO<sub>3</sub><sup>-</sup> > Cl<sup>-</sup> > NO<sub>3</sub><sup>-</sup> and Ca<sup>++</sup> > Na<sup>+</sup> > Mg<sup>++</sup> > K<sup>+</sup>. Sulphates (SO<sub>4</sub><sup>-2</sup>) and calcium (Ca) are the most common ions among anions and cations. Thus, these parameters can be tested to save time, money, and energy in routine examinations while producing acceptable results if other param-

**Table 5** Pearson correlation coefficient of the analysed groundwater quality parameters

	<i>PH</i>	<i>EC</i>	<i>TDS</i>	<i>NO<sub>3</sub></i>	<i>SO<sub>4</sub></i>	<i>CL</i>	<i>HCO<sub>3</sub></i>	<i>TH</i>	<i>CA</i>	<i>MG</i>	<i>NA</i>	<i>K</i>	<i>WQI</i>
<i>PH</i>	1												
<i>EC</i>	0.150	1											
<i>TDS</i>	0.219	0.886	1										
<i>NO<sub>3</sub></i>	-0.007	-0.088	-0.093	1									
<i>SO<sub>4</sub></i>	0.189	0.580	0.794	-0.060	1								
<i>CL</i>	0.181	0.401	0.629	-0.113	0.428	1							
<i>HCO<sub>3</sub></i>	-0.311	0.044	0.013	-0.277	-0.009	0.068	1						
<i>TH</i>	0.231	0.740	0.880	0.022	0.872	0.586	-0.026	1					
<i>CA</i>	0.167	0.669	0.828	0.068	0.842	0.543	-0.072	0.948	1				
<i>MG</i>	0.283	0.688	0.768	-0.058	0.724	0.524	0.055	0.859	0.653	1			
<i>NA</i>	0.204	0.444	0.715	-0.173	0.673	0.850	0.103	0.609	0.567	0.540	1		
<i>K</i>	-0.048	0.494	0.483	-0.100	0.320	0.221	0.064	0.356	0.306	0.357	0.246	1	
<i>WQI</i>	0.190	0.801	0.939	0.101	0.882	0.639	0.088	0.927	0.874	0.805	0.741	0.482	1

-1                      0                      1

Values close to 1 and - 1: high correlation; values close to 0: low correlation

eters are not available. In fact, our study depicts limitations because of the lack of microbiological analysis data and the difficult access to boreholes in the Algerian-Moroccan borders.

- (ii) The groundwater in the studied watershed depicts a Ca-Mg-SO<sub>4</sub>-Cl type as stated by piper's trilinear diagram. The Gibbs plot highlights that most of the samples fell into the field of dominant rock-water interaction. Therefore, the geology where the groundwater is located is the key element which controls the chemical groundwater composition. Other factors influencing water quality are the type of rocks, the geological formation, and the weathering process occurring in the region. The Berrasian formations, characterised by many evaporite minerals, depict problems of high-water salinity. The formation of these evaporites was caused by the contaminated water from the adjoining aquifers. The best quality water among the analysed groundwater samples belongs to the Albian formations. Therefore, local authorities should stop drilling wells in the Berrasian formations.
- (iii) The groundwater classification, based on the WQI, has shown that 20.9% of the water samples are of excellent quality, 69.8% are of good quality and 9.3% are of poor quality. Likewise, to distribute major ions in the study region and to assess the spatial distribution of drinking water quality, the IDW interpolation

technique was used. Thus, integrating WQI and GIS allows creating of maps to represent the spatial distribution of water quality parameters, based on the analysis of data extracted at different stages of operation. This research has contributed to understanding the physic-chemical properties of water in the Ain Sefra basin. The outcome of this research work can be used by policy-makers, and local and regional authorities, to improve groundwater management and offer safe drinking water to all populations in arid and semi-arid areas.

**Supplementary Information** The online version contains supplementary material available at <https://doi.org/10.1007/s12665-023-11183-9>.

**Acknowledgements** The researchers would like to acknowledge the Deanship of Scientific Research, Taif University for funding this work. Antonio Jodar-Abellan acknowledges financial support received from the Margarita Salas postdoc Spanish Program. In the same way, the authors acknowledge the reviewers and editor of this manuscript whose comments contributed greatly to improve this paper.

**Author contributions** A. Derdour: Conceptualization, methodology, software, formal analysis, data curation, writing (original draft), funding acquisition. A. Jodar: Conceptualization, methodology, formal analysis, writing review and editing, funding acquisition. M.A. Pardo: Conceptualization, methodology, formal analysis, writing review and editing, funding acquisition. S. Ghoneim: Conceptualization, formal analysis, writing review and editing, funding acquisition. A. Almaiki: writing review and editing, funding acquisition. E. Hussein: writing

review and editing. All authors provided critical feedback and helped to shape the research, analysis, and approved the final version of the manuscript.

**Funding** Open Access funding provided thanks to the CRUE-CSIC agreement with Springer Nature.

**Availability of data and materials** The data presented in this study are available on request from the first or corresponding authors.

## Declarations

**Conflict of interest** The authors declare no conflict of interest.

**Ethical approval** Not applicable.

**Consent to publish** Not applicable.

**Consent to participate** Not applicable.

**Open Access** This article is licensed under a Creative Commons Attribution 4.0 International License, which permits use, sharing, adaptation, distribution and reproduction in any medium or format, as long as you give appropriate credit to the original author(s) and the source, provide a link to the Creative Commons licence, and indicate if changes were made. The images or other third party material in this article are included in the article's Creative Commons licence, unless indicated otherwise in a credit line to the material. If material is not included in the article's Creative Commons licence and your intended use is not permitted by statutory regulation or exceeds the permitted use, you will need to obtain permission directly from the copyright holder. To view a copy of this licence, visit <http://creativecommons.org/licenses/by/4.0/>.

## References

- Achilleos G (2011) The inverse distance weighted interpolation method and error propagation mechanism-creating a DEM from an analogue topographical map. *J J Spatial Sci* 56(2):283–304. <https://doi.org/10.1080/14498596.2011.623348>
- Al-Dulaimi GA, Younes MK (2017) Assessment of potable water quality in Baghdad City, Iraq. *J Air Soil Water Res*. <https://doi.org/10.1177/1178622117733441>
- Annan K (2005) In larger freedom: decision time at the UN. *J Foreign Aff*. 84:63. <https://www.un.org/sg/en/content/sg/articles/2005-04-25/larger-freedom-decision-time-un>. Accessed 25 Jan 2022
- ArcGIS (2020) ArcGIS 10.6 (Geographic Information System). Retrieved from <https://support.esri.com/es/downloads>. Accessed 23 Mar 2022
- Arega T (2020) Sodium and potassium analysis of drinking water quality assessment and its health effects in Ethiopia: a retrospective study. *J Oral Health Dentistry* 4(1):261–266
- Asadollah SBH, Sharafati A, Motta D, Jodar-Abellan A, Pardo MA (2023) Satellite-based prediction of surface dust mass concentration in southeastern Iran using an intelligent approach. *Stoch Env Res Risk Assess*. <https://doi.org/10.1007/s00477-023-02473-6>
- Bancessi A, Catarino L, José Silva M, Ferreira A, Duarte E, Nazareth T (2020) Quality assessment of three types of drinking water sources in Guinea-Bissau. *J Int J Environ Res Public Health* 17(19):7254. <https://doi.org/10.3390/ijerph17197254>
- Baudron P (2013) Anthropization of a semiarid Mediterranean multi-layer aquifer system (Campo de Cartagena, SE Spain): hydrodynamic, geochemical and isotopic approaches. *Universidad de Murcia Université Montpellier II-Sciences et Techniques du Languedoc, Murcia*
- Bendida A, Kendouci MA, Tidjani AEB (2021) Characterization of Algerian Sahara groundwater for irrigation and water supply: Adrar region study case. *J Water Land Dev*. <https://doi.org/10.24425/jwld.2021.137117>
- Boansi-Okofo L, Akyeref-Anderson N, Bedu-Addo K, Afrakoma-Armoo E (2021) Hydrochemical peculiarities and groundwater quality assessment of the Birimian and Tarkwaian aquifer systems in Bosome Freho District and Bekwai Municipality of the Ashanti Region. *Ghana Environ Earth Sci* 80:818. <https://doi.org/10.1007/s12665-021-10081-2>
- Boix-Fayos C, Boerboom L, Janssen R, Martínez M, Almagro M, Pérez P, Eekhout J, Castillo V, de Vente J (2020) Mountain ecosystem services affected by land use changes and hydrological control works in Mediterranean catchments. *Ecosyst Serv*. <https://doi.org/10.1016/j.ecoser.2020.101136>
- Bouarfa S, Bellal SA (2018) Assessment of the Aeolian sand dynamics in the region of Ain Sefra (Western Algeria), using wind data and satellite imagery. *J Arabian J Geosci* 11(3):1–16. <https://doi.org/10.1007/s12517-017-3346-9>
- Brown RM, McClelland NI, Deininger RA, O'Connor MF (1972) A water quality index-crashing the psychological barrier. *Indicators of environmental quality*. Springer, New York, pp 173–182. [https://doi.org/10.1007/978-1-4684-2856-8\\_15](https://doi.org/10.1007/978-1-4684-2856-8_15)
- Canada H (2008) Guidance for potassium from water softeners. Ottawa, Ontario, Health Canada, Healthy Environments and Consumer Safety Branch, Water, Air and Climate Change Bureau Retrieved from <http://www.hc-sc.gc.ca/ewh-semt/pubs/water-eau/potassium/index-eng.php>. Accessed 19 Feb 2022
- Chabuk A, Al-Madhloom Q, Al-Maliki A, Al-Ansari N, Hussain HM, Laue J (2020) Water quality assessment along Tigris River (Iraq) using water quality index (WQI) and GIS software. *Arab J Geosci* 13:1–23. <https://doi.org/10.1007/s12517-020-05575-5>
- Chakraborty B, Roy S, Bera A, Adhikary PP, Bera B, Sengupta D, Shit PK (2021) Geospatial assessment of groundwater quality for drinking through water quality index and human health risk index in an upland area of Chota Nagpur Plateau of West Bengal, India. *Spatial modeling and assessment of environmental contaminants*. Springer, New York, pp 327–358. [https://doi.org/10.1007/978-3-030-63422-3\\_19](https://doi.org/10.1007/978-3-030-63422-3_19)
- Charizopoulos N, Zagana E, Psilovikos A (2018) Assessment of natural and anthropogenic impacts in groundwater, utilizing multivariate statistical analysis and inverse distance weighted interpolation modeling: the case of a Scopia basin (Central Greece). *Environ Earth Sci* 77:380. <https://doi.org/10.1007/s12665-018-7564-6>
- Damo R, Icka P (2013) Evaluation of Water Quality Index for Drinking Water. *J Polish J Environ Stud* 22(4):1045–1051
- Davie MG, Cheng H, Hopkins GD, Lebron CA, Reinhard M (2008) Implementing heterogeneous catalytic dechlorination technology for remediating TCE-contaminated groundwater. *J Environ Sci Technol* 42(23):8908–8915. <https://doi.org/10.1021/es8014919>
- de Almeida GS, de Oliveira IB (2018) Application of the index WQI-CCME with data aggregation per monitoring campaign and per section of the river: case study-Joanes River. *Brazil J Environ Monit Assess* 190(4):1–20. <https://doi.org/10.1007/s10661-018-6542-5>
- de Vente J, Verduyn R, Verstraeten G, Vanmaercke M, Poesen J (2011) Factors controlling sediment yield at the catchment scale in NW Mediterranean geoecosystems. *J Soils Sediment* 11:690–707. <https://doi.org/10.1007/s11368-011-0346-3>
- Derdour A, Bouanani A (2019) Coupling HEC-RAS and HEC-HMS in rainfall-runoff modeling and evaluating floodplain inundation maps in arid environments: case study of Ain Sefra city, Ksour



- Mountain SW of Algeria. *J Environ Earth Sci* 78(19):1–17. <https://doi.org/10.1007/s12665-019-8604-6>
- Derdour A, Chabane Sari S (2020) Evaluation of the quality of groundwater for its appropriateness for drinking purposes in the watershed of Naama, SW of Algeria, by using water quality index (WQI). *J SN Appl Sci* 2(12):1–14. <https://doi.org/10.1007/s42452-020-03768-x>
- Derdour A, Bouanani A, Babahamed K (2018) Modelling rainfall runoff relations using HEC-HMS in a semi-arid region: case study in Ain Sefra watershed, Ksour Mountains (SW Algeria). *J J Water Land Dev*. <https://doi.org/10.2478/jwld-2018-0005>
- Derdour A, Guerine L, Allali M (2021) Assessment of drinking and irrigation water quality using WQI and SAR method in Maâder sub-basin, Ksour Mountains, Algeria. *J Sustain Water Resour Manag* 7(1):1–14. <https://doi.org/10.1007/s40899-021-00490-3>
- Derdour A, Bouanani A, Kaid N, Mukdasai K, Algelany A, Ahmad H, Ameur H (2022) Groundwater potentiality assessment of Ain Sefra region in upper Wadi Namous Basin, Algeria using integrated geospatial approaches. *Sustainability*. 14(8):4450. <https://doi.org/10.3390/su14084450>
- Desye B, Belete B, Asfaw Gebrezgi Z, Terefe Reda T (2021) Efficiency of treatment plant and drinking water quality assessment from source to household, Gondar city, northwest Ethiopia. *J J Environ Publ Health*. <https://doi.org/10.1155/2021/9974064>
- Djidi K, Bakalowicz M, Benali AM (2008) Mixed, classical and hydrothermal karstification in a carbonate aquifer: hydrogeological consequences. The case of the Saida aquifer system Algeria. *Comptes Rendus Geosci* 340(7):462–473. <https://doi.org/10.1016/j.crte.2008.04.002>
- Eekhout J, Millares A, Martínez A, García R, Pérez P, Conesa C, de Vente J (2021) A process-based soil erosion model ensemble to assess model uncertainty in climate change impact assessments. *Land Degrad Dev* 32:2409–2422. <https://doi.org/10.1002/ldr.3920>
- El Behairy RA, El Baroudy AA, Ibrahim MM, Kheir AM, Shokr MS (2021) Modelling and assessment of irrigation water quality index using GIS in semi-arid region for sustainable agriculture. *Water Air Soil Pollut* 232(9):352. <https://doi.org/10.1007/s11270-021-05310-0>
- El Osta M, Niyazi B, Masoud M (2022) Groundwater evolution and vulnerability in semi-arid regions using modeling and GIS tools for sustainable development: case study of Wadi Fatimah. *Saudi Arabia Environ Earth Sci* 81:248. <https://doi.org/10.1007/s12665-022-10374-0>
- García-López M, Montano B, Melgarejo J (2022) The tariff structure in the Tagus-Segura water transfer. *Water* 14:413. <https://doi.org/10.3390/w14030413>
- Gibbs RJ (1970) Mechanisms controlling world water chemistry. *J Sci* 170(3962):1088–1090. <https://doi.org/10.1126/science.170.3962.1088>
- Gradilla-Hernández MS, de Anda J, Garcia-Gonzalez A, Montes CY, Barrios-Piña H, Ruiz-Palomino P, Díaz-Vázquez D (2020) Assessment of the water quality of a subtropical lake using the NSF-WQI and a newly proposed ecosystem specific water quality index. *J Environ Monit Assess* 192(5):1–19. <https://doi.org/10.1007/s10661-020-08265-7>
- Hamlat A, Guidoum A (2018) Assessment of groundwater quality in a semiarid region of Northwestern Algeria using water quality index (WQI). *Appl Water Sci* 8(8):220. <https://doi.org/10.1007/s13201-018-0863-y>
- Hamzah Z, Wan Rosdi WN, Wood AK, Saat A (2014) Determination of major ions concentrations in Kelantan well water using EDXRF and ion chromatography. *J Malaysian J Analytical Sci* 18(1):178
- Hartmann A, Barberá JA, Lange J, Andreo B, Weiler M (2013) Progress in the hydrologic simulation of time variant recharge areas of karst systems-exemplified at a karst spring in Southern Spain. *J Adv Water Resour* 54:149–160. <https://doi.org/10.1016/j.advwatres.2013.01.010>
- Hinge G, Bharali B, Baruah A et al (2022) Integrated groundwater quality analysis using Water Quality Index, GIS and multivariate technique: a case study of Guwahati City. *Environ Earth Sci* 81:412. <https://doi.org/10.1007/s12665-022-10544-0>
- Hornero-Díaz JE (2018) Contribución de las técnicas hidroquímicas, isotópicas e hidrodinámicas a la caracterización de acuíferos carbonatados y su relación con la red de flujo superficial. Aplicación al acuífero de Alcadozo (cuenca del Segura). (Doctoral Thesis), Universidad Politécnica de Cartagena.
- Horton J, Hawkins R (1965) Flow path of rain from the soil surface to the water table. *J Soil Science* 100(6):377–383
- Institute for Health Metrics and Evaluation (IHME) (2015) GBD Compare. Retrieved from <http://vizhub.healthdata.org/gbd-compare> Accessed 12 Feb 2022
- Jehan S, Ullah I, Khan S, Muhammad S, Khattak SA, Khan T (2020) Evaluation of the Swat River, Northern Pakistan, water quality using multivariate statistical techniques and water quality index (WQI) model. *J Environ Sci Pollut Res* 27(31):38545–38558. <https://doi.org/10.1007/s11356-020-09688-y>
- Jodar-Abellan A, Valdes-Abellan J, Pla C, Gomariz-Castillo F (2019) Impact of land use changes on flash flood prediction using a sub-daily SWAT model in five Mediterranean ungauged watersheds (SE Spain). *J Sci Total Environ* 657:1578–1591. <https://doi.org/10.1016/j.scitotenv.2018.12.034>
- JORADP (2011) Executive Decree No. 11–125 of March 22, 2011 on the quality of water for human consumption in Algeria. *JORADP* (Official Journal of the Algerian Republic).
- Kanagaraj G, Elango L (2016) Hydrogeochemical processes and impact of tanning industries on groundwater quality in Ambur, Vellore district, Tamil Nadu. *India J Environ Sci Pollut Res* 23(23):24364–24383. <https://doi.org/10.1007/s11356-016-7639-4>
- Karandish F, Hoekstra AY, Hogeboom RJ (2018) Groundwater saving and quality improvement by reducing water footprints of crops to benchmarks levels. *J Adv Water Res* 121:480–491. <https://doi.org/10.1016/j.advwatres.2018.09.011>
- Kawo NS, Karuppappan S (2018) Groundwater quality assessment using water quality index and GIS technique in Modjo River Basin, central Ethiopia. *J Afr Earth Sc* 147:300–311. <https://doi.org/10.1016/j.jafrearsci.2018.06.034>
- Kendouci MA, Bendida A, Mebarki S, Kharroubi B (2019) Study of the management efficiency of the drinking water supply in arid areas: case of Bechar city (southwest of Algeria). *J Appl Water Sci* 9(8):1–7. <https://doi.org/10.1007/s13201-019-1081-y>
- Kumar A, Kumar V, Pandita S, Singh S, Bhardwaj R, Varol M, Rodrigo-Comino J (2023) A global meta-analysis of toxic metals in continental surface water bodies. *J Environ Chem Eng*. 11(3):109964. <https://doi.org/10.1016/j.jece.2023.109964>
- Latha PS (2022) Evaluation of groundwater quality for domestic and irrigation purposes in a coastal alluvial aquifer using multivariate statistics and entropy water quality index approach: a case study from West Godavari Delta, Andhra Pradesh (India). *Environ Earth Sci* 81:275. <https://doi.org/10.1007/s12665-022-10387-9>
- Li C, Gao Z, Chen H et al (2021) Hydrochemical analysis and quality assessment of groundwater in southeast North China Plain using hydrochemical, entropy-weight water quality index, and GIS techniques. *Environ Earth Sci* 80:523. <https://doi.org/10.1007/s12665-021-09823-z>
- Long A, Yu J, He X, Deng X, Su S, Zhang J, Hai Y (2021) Linking local water consumption in inland arid regions with imported virtual water: approaches, application and actuators. *J Adv Water Res*. 151:103906. <https://doi.org/10.1016/j.advwatres.2021.103906>

- Lumb A, Sharma T, Bibeault JF (2011) A review of genesis and evolution of water quality index (WQI) and some future directions. *J Water Qual Expo Health* 3(1):11–24. <https://doi.org/10.1007/s12403-011-0040-0>
- Maleika W (2020) Inverse distance weighting method optimization in the process of digital terrain model creation based on data collected from a multibeam echosounder. *J Appl Geomat* 12(4):397–407. <https://doi.org/10.1007/s12518-020-00307-6>
- Mansouri Z, Leghrie Y, Kouadri S, Al-Ansari N, Najm HM, Mashaan NS, Khedher KM (2022) Hydro-geochemistry and groundwater quality assessment of Ouargla basin, South of Algeria. *Water* 14(15):2441. <https://doi.org/10.3390/w14152441>
- Melalih A, Mazour M (2021) Analysis of water and soil conservation techniques at the Ain Sefra arid watershed (Ksour Mountains, southwest Algeria). *J Environ Monit Assess* 193(1):1–18. <https://doi.org/10.1007/s10661-020-08842-w>
- Meride Y, Ayenew B (2016) Drinking water quality assessment and its effects on residents health in Wondo genet campus Ethiopia. *J Environ Syst Res* 5(1):1–7. <https://doi.org/10.1186/s40068-016-0053-6>
- Morr S, Cuartas E, Alwattar B, Lane JM (2006) How much calcium is in your drinking water? A survey of calcium concentrations in bottled and tap water and their significance for medical treatment and drug administration. *J HSS Journal* 2(2):130–135. <https://doi.org/10.1007/s11420-006-9000-9>
- Moussaoui T, Derdour A, Hosni A, de Ballesta Los Santos M, Legua P, Pardo-Picazo MA (2023) Assessing the quality of treated wastewater for irrigation: a case study of Ain Sefra wastewater treatment plant. *Sustainability*. 15:11133. <https://doi.org/10.3390/su151411133>
- Nath B, Ni-Meister W, Choudhury R (2021) Impact of urbanization on land use and land cover change in Guwahati city, India and its implication on declining groundwater level. *J Groundw Sustain Dev* 12:100500. <https://doi.org/10.1016/j.gsd.2020.100500>
- Nerbrand C, Agréus L, Lenner RA, Nyberg P, Svärdsudd K (2003) The influence of calcium and magnesium in drinking water and diet on cardiovascular risk factors in individuals living in hard and soft water areas with differences in cardiovascular mortality. *J BMC Public Health* 3(1):1–9. <https://doi.org/10.1186/1471-2458-3-21>
- Nong X, Shao D, Zhong H, Liang, J.J.W.r. (2020) Evaluation of water quality in the South-to-North Water Diversion Project of China using the water quality index (WQI) method. *J Water Res.* 178:115781. <https://doi.org/10.1016/j.watres.2020.115781>
- Pardo M, Navarro-Gonzalez F, Villacampa Y (2022) An algorithm to schedule water delivery in pressurized irrigation networks. *J Comput Electron Agric.* 201:107290. <https://doi.org/10.1016/j.compag.2022.107290>
- Piper AM (1944) A graphic procedure in the geochemical interpretation of water-analyses. *J Eos, Trans Am Geophys Union* 25(6):914–928. <https://doi.org/10.1029/TR025i006p00914>
- Pla C, Benavente D, Valdes-Abellan J, Kovacova Z (2021) Effectiveness of two lightweight aggregates for the removal of heavy metals from contaminated urban stormwater. *J Contam Hydrol.* 239:103778. <https://doi.org/10.1016/j.jconhyd.2021.103778>
- Prüss-Ustün A, Wolf J, Bartram J, Clasen T, Cumming O, Freeman MC, Johnston R (2019) Burden of disease from inadequate water, sanitation and hygiene for selected adverse health outcomes: an updated analysis with a focus on low-and middle-income countries. *J Int J Hygiene Environ Health* 222(5):765–777. <https://doi.org/10.1016/j.ijheh.2019.05.004>
- Rabeiy RE (2018) Assessment and modeling of groundwater quality using WQI and GIS in Upper Egypt area. *J Environ Sci Pollut Res* 25(31):30808–30817. <https://doi.org/10.1007/s11356-017-8617-1>
- Rahmani A, Bouanani A, Kacemi A, Hamed KB (2017) Contribution of GIS for the survey and the management of water resources in the basin “Benhandjir–Tirkount”(Ain Sefra)–mounts of Ksour-Saharan Atlas-Algeria. *J J Fundam Appl Sci* 9(2):829–846. <https://doi.org/10.4314/JFAS.V9I2.14>
- Ramos MAG, de Bueno Oliveira ES, Pião ACS, de Nalin Oliveira Leite DA, de Franceschi Angelis D (2016) Water quality index (WQI) of Jaguari and Atibaia Rivers in the region of Paulínia, São Paulo Brazil. *J Environ Monit Assess* 188(5):1–14. <https://doi.org/10.1007/s10661-016-5261-z>
- Rao GS, Nageswararao G (2013) Assessment of ground water quality using water quality index. *Arch Environ Sci* 7(1):1–5
- Rapant S, Cvečková V, Fajčíková K, Sedláková D, Stehlíková B (2017) Impact of calcium and magnesium in groundwater and drinking water on the health of inhabitants of the Slovak Republic. *J Int J Environ Res Publ Health* 14(3):278. <https://doi.org/10.3390/ijerph14030278>
- Russell AF (2010) International organizations and human rights: realizing, resisting or repackaging the right to water? *J Human Rights* 9(1):1–23. <https://doi.org/10.1080/14754830903530292>
- Sadat-Noori S, Ebrahimi K, Liaghat A (2014) Groundwater quality assessment using the Water Quality Index and GIS in Saveh-Nobaran aquifer. *Iran J Environ Earth Sci* 71(9):3827–3843. <https://doi.org/10.1007/s12665-013-2770-8>
- Sarath-Prasanth S, Magesh N, Jitheshlal K, Chandrasekar N, Gangadhar K (2012) Evaluation of groundwater quality and its suitability for drinking and agricultural use in the coastal stretch of Alappuzha District, Kerala. *India J Appl Water Sci* 2(3):165–175. <https://doi.org/10.1007/s13201-012-0042-5>
- Scheelbeek PF, Chowdhury MA, Haines A, Alam DS, Hoque MA, Butler AP, Elliott P (2017) Drinking water salinity and raised blood pressure: evidence from a cohort study in coastal Bangladesh. *J Environ Health Perspect* 125(5):057007. <https://doi.org/10.1289/EHP659>
- Shepard D (1968) A two-dimensional interpolation function for irregularly-spaced data. *Proceedings of the 1968 ACM National Conference.* p 517–524. <https://doi.org/10.1145/800186.810616>
- Song C, Yao L (2022) A hybrid model for water quality parameter prediction based on CEEMDAN-IALO-LSTM ensemble learning. *Environ Earth Sci* 81:262. <https://doi.org/10.1007/s12665-022-10380-2>
- Tajmunnaher T, Chowdhury MAI (2017) Correlation study for assessment of water quality and its parameters of Kushiyara River, Sylhet, Bangladesh. *Int J New Technol Res* 3(12):263179. <https://www.ijntr.org/correlation-study-for-assessment-of-water-quality-and-its-parameters-of-kushiyara-river-sylhet-bangladesh>
- Tian L, Wu W, Zhou X, Zhang D, Yu Y, Wang H, Wang Q (2019) The ecosystem effects of Sand-Binding Shrub *Hippophae rhamnoides* in Alpine Semi-Arid Desert in the Northeastern Qinghai-Tibet Plateau. *J Land* 8(12):183. <https://doi.org/10.3390/land8120183>
- Valdes-Abellan J, Pardo M, Jódar-Abellán A, Pla C, Fernandez-Mejuto M (2020) Climate change impact on karstic aquifer hydrodynamics in southern Europe semi-arid region using the KAGIS model. *J Sci Total Environ.* 723:138110. <https://doi.org/10.1016/j.scitotenv.2020.138110>
- Wada Y, van Beek LP, Bierkens MF (2012) Nonsustainable groundwater sustaining irrigation: a global assessment. *J Water Res Res.* <https://doi.org/10.1029/2011WR010562>
- Wang X, Zhang F (2018) Multi-scale analysis of the relationship between landscape patterns and a water quality index (WQI) based on a stepwise linear regression (SLR) and geographically weighted regression (GWR) in the Ebinur Lake oasis. *J Environ Sci Pollut Res* 25(7):7033–7048. <https://doi.org/10.1007/s11356-017-1041-8>
- WHO (2011) Guidelines for drinking-water quality 38(4):104–108. <https://www.who.int/publications/i/item/9789241549950>. Accessed 1 Mar 2022

Yang CY (1998) Calcium and magnesium in drinking water and risk of death from cerebrovascular disease. *J Stroke* 29(2):411–414. <https://doi.org/10.1161/01.str.29.2.411>

**Publisher's Note** Springer Nature remains neutral with regard to jurisdictional claims in published maps and institutional affiliations.